JCTC Journal of Chemical Theory and Computation

Study of the Topological Properties of Some Pseudohalides

Nora B. Okulik,[†] Alicia H. Jubert,[‡] and Eduardo A. Castro*[,§]

Facultad de Agroindustrias, UNNE, Cte. Fernández 755, 3700 Pcia. R. Sáenz Peña, Chaco, Argentina, and CEQUINOR, Departamento de Química, Facultad de Ciencias Exactas 47 y 115 y Facultad de Ingeniería 1 y 47 and INIFTA, Departamento de Química, Facultad de Ciencias Exactas, Universidad Nacional de La Plata, 1900 Buenos Aires, Argentina

Received December 3, 2005

Abstract: The pseudohalide principle has been used extensively in nonmetal chemistry to predict the structure and stability of many molecular species. The 1,2,3,4-thiatriazole-5-thiolate anion, $CS_2N_3^-$, is of particular interest. In a short communication we have recently reported the topological study of some $CS_2N_3^-$containing species reported by Crawford et al. Previous reports on these compounds showed that in covalent derivatives not only does the ring remain intact but also the site of attachment of the R group is most likely at the exocyclic sulfur atom in contrast to the previously suggested N−R connectivity. Therefore, the structure and bonding of derivatives of the $CS_2N_3^-$ moiety is clearly an important question. With that in our mind, we undertook a topological analysis, based on the AIM theory, to gain more insight into the bonding in covalent derivatives of the $CS_2N_3^-$ moiety, trying to find an explanation to the origin of the N−H and S−H connectivities. The question is which is the reason that makes all the covalent derivatives prefer the S−R connectivity while the hydracid has an N−H one.

Introduction

The study of pseudohalides has been of interest to nonmetal chemists for many years. Due to the similarities between the halides and the pseudohalides, the pseudohalide family of compounds is of fundamental chemical interest.[1] The pseudohalide concept was introduced in 1925,[2] and since its introduction, the pseudohalide principle has been used extensively in nonmetal chemistry to predict the structure and stability of many species.

The so-called "azidodithiocarbonate" anion, more properly referred to as the 1,2,3,4-thiatriazole-5-thiolate anion, $CS_2N_3^-$, is of particular interest.[3] First described and isolated in 1918 by Sommer,[4] it was not until 1991 that the structure of the $CS_2N_3^-$ anion in the form of its $NaCS_2N_3{\cdot}2H_2O$ salt was determined experimentally using X-ray diffraction techniques to be a five-membered ring,[5] in contrast to the previously postulated chain structure.[4] While early reports suggested the formation of several derivatives of this anion, little or no data were presented to support these claims.[6]

Crawford et al. have reported the characterization of several $CS_2N_3^-$ containing species.[3,7] They also reported the quantum-chemical calculations on the $CS_2N_3^-$ moiety which not only supported the formation of the five-membered ring but also were also in a very good agreement with the experimentally determined structure.[5] In a short communication we have recently reported the topological study of any $CS_2N_3^-$ containing species reported by Crawford et al.[8]

A previous report on these compounds showed that in covalent derivatives[5] not only did the ring remain intact but also the site of attachment of the R group is most likely at the exocyclic sulfur atom in contrast to the previously suggested N−R connectivity.[9] Therefore, the structure and bonding of derivatives of the $CS_2N_3^-$ moiety is clearly an important question. With that in our mind, we undertook a topological analysis to gain more insight into the bonding

* Corresponding author e-mail: castro@quimica.unlp.edu.ar.
[†] UNNE.
[‡] CEQUINOR.
[§] INIFTA.

10.1021/ct0503062 CCC: $33.50
Published on Web 07/20/2006

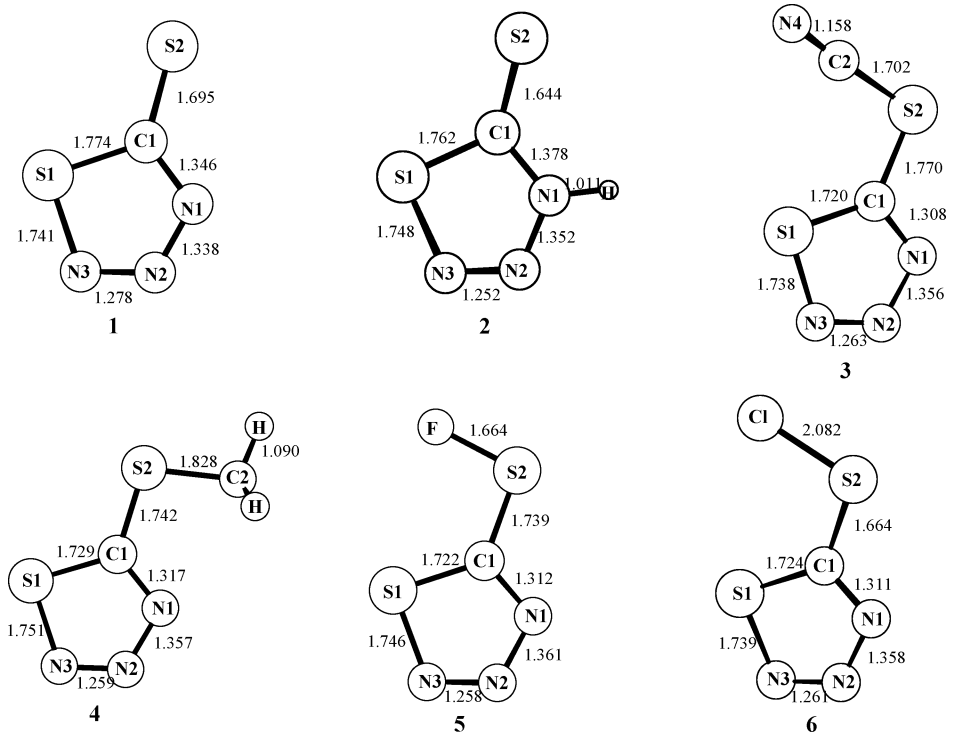

Figure 1. Optimized structures of 1,2,3,4-thiatriazole-5-thiolate anion, $CS_2N_3^-$ (**1**), hydracid, $HN_3SC{=}S$ (**2**), interpseudohalogen, $CS_2N_3{-}CN$ (**3**), methylazidodithiocarbonate, $CH_3CS_2N_3$ (**4**), chloroazidodithiocarbonate, $ClCS_2N_3$ (**5**), and fluoroazidodithiocarbonate, FCS_2N_3 (**6**), calculated at the B3LYP/6-311++G* level. The atomic labeling scheme and the bond lengths are indicated.

in covalent derivatives of the $CS_2N_3^-$ moiety, trying to find an explanation to the origin of the N−H and S−H connectivities. The question is what is the reason that makes all the covalent derivatives prefer the S−R connectivity while the hydracid has an N−H one.

Methods of Calculation and Computational Details

The structures of pseudohalides were calculated using the density functional theory,[10] and their topological properties are analyzed in terms of the atoms-in-molecules (AIM) method.[11] All calculations were carried out using the Gaussian 98 package.[12] The Becke's three-parameter density functional[13] together with the Lee, Yang, and Parr functional, which accounts for both local and gradient-corrected correlation effects,[14] were used to accomplish the calculations. This combination leads to the well-known and widely used B3LYP method. The basis set used for all elements was 6-311++G*.[15] Each optimized structure was tested against imaginary frequencies in order to be sure they are located at an energy minimum.

The topological analysis of all the species under study was accomplished by means of the PROAIM program.[16] The densities used for the topological analysis were obtained through single-point calculations on the above optimized geometries using the B3LYP level of theory and the 6-311++G** basis set provided by the Gaussian 98 package.[12]

Atoms-in-Molecules Theory: An Overview. The AIM theory is a simple, rigorous, and elegant way of defining atoms and bonds within a chemical structure. This theory is based on the critical points (CP) of the electronic density, $\rho(\mathbf{r})$. These are points where the gradient of the electronic density, $\nabla\rho(\mathbf{r})$, vanishes, and they are characterized by the three eigenvalues (λ_1, λ_2, λ_3) of the Hessian matrix of $\rho(\mathbf{r})$. The CPs are labeled as (r, s) according to their rank, r (number of nonzero eigenvalues), and signature, s (the algebraic sum of the signs of the eigenvalues).

Four types of CPs are of interest in molecules: (3, −3), (3,−1), (3, +1), and (3, +3). A (3, −3) point corresponds to a maximum in $\rho(\mathbf{r})$, and it appears generally at the nuclear positions. A (3, +3) point indicates electronic charge depletion and is known as a cage critical point. (3, +1) points, or ring critical points, are merely saddle points. Finally, a (3, −1) point, or bond critical point, is generally found between two neighboring nuclei indicating the existence of a bond between them.

Several properties that can be evaluated at the bond critical point, BCP, constitute very powerful tools to classify the interactions between two fragments.[11] Calculated properties at the BCP of the electronic density are labeled with the subscript "b" throughout the work.

The two negative eigenvalues of the Hessian matrix (λ_1 and λ_2) at the BCP measure the degree of contraction of ρ_b perpendicular to the bond toward the critical point, while the positive eigenvalue (λ_3) measures the degree of contraction parallel to the bond and from the BCP toward each of the neighboring nuclei. When the negative eigenvalues dominate, the electronic charge is locally concentrated within the region of the BCP leading to an interaction characteristic typically found in covalent or polarized bonds and being characterized by large ρ_b values, $\nabla^2\rho_b < 0$, $|\lambda_1|/\lambda_3 > 1$, and $G_b/\rho_b < 1$, with G_b being the local kinetic energy density at the bond critical point. On the other hand, if the positive

Table 1: Comparison of Selected Experimentally Determined (X-ray) and Calculated (B3LYP/6-311++G*) Structural Parameters (Å, deg) for **1**−**6** Structures

	1		**2**		**3**		**4**		**5**		**6**	
parameter[a]	calc	exptl[b]	calc	exptl[b]	calc	exptl[b]	calc	exptl[c]	calc	calc[d]	calc	calc[e]
C_1-S_2	1.695	1.696	1.644	1.661	1.770	1.756	1.742	1.723	1.739	1.739	1.664	1.72
C_1-N_1	1.346	1.340	1.378	1.346	1.308	1.305	1.317	1.314	1.312	1.312	1.311	1.31
C_1-S_1	1.774	1.717	1.762	1.722	1.720	1.699	1.729	1.699	1.722	1.722	1.724	1.75
N_1-N_2	1.338	1.347	1.352	1.351	1.356	1.364	1.357	1.356	1.361	1.361	1.358	1.36
N_2-N_3	1.278	1.286	1.252	1.260	1.263	1.276	1.259	1.274	1.258	1.258	1.261	1.26
S_1-N_3	1.741	1.682	1.748	1.706	1.738	1.670	1.751	1.680	1.746	1.747	1.739	1.74
N_1-H			1.011	0.800								
S_2-C_2					1.702	1.697	1.828	1.799				
C_2-N_4					1.158	1.139						
C_2-H							1.090	0.92				
S_2-X									1.664	1.663	2.082	2.08
$S_1-C_1-N_1$	108.0	109.1	103.2	105.2	113.2	112.7	112.2	111.8	113.5	113.5	112.9	112.9
$S_2-C_1-S_1$	124.3	124.3	130.3	127.65	129.5	124.6	123.4	122.3	127.6	127.5	129.8	129.8
$C_1-S_1-N_3$	90.5	91.7	92.2	92.03	87.9	89.5	88.3	89.9	87.6	87.5	87.9	87.0
$N_1-N_2-N_3$	118.7		113.7		117.0		117.8	116.6	117.2	117.2	117.0	117.1
C_1-N_1-H			122.6	120.0								
$S_2-C_2-N_4$					176.3	172.6						
C_1-S_2-X									98.2	98.2	101.5	101.5

[a] See Figure 1 for labels. [b] Reference 7c. [c] Reference 3. [d] Reference 7a. [e] Reference 7b.

eigenvalue is dominant, the electronic density is locally concentrated at each atomic site. The interaction is now referred to as a closed-shell one, and it is characteristic of highly ionic bonds, hydrogen bonds, and van der Waals interactions. It is characterized by relatively low ρ_b values, $\nabla^2\rho_b > 0$, $|\lambda_1|/\lambda_3 < 1$, and $G_b/\rho_b > 1$. Finally, the ellipticity, ϵ, defined as $\lambda_1/\lambda_2 - 1$ indicates the deviation of the electronic charge density from the axial symmetry of a chemical bond providing a quantitative measure of the π character of the bond or of the delocalization electronic charge.

Other properties are obtained by integrating the corresponding property density over the atomic basin, which is denoted by Ω.[11] The relevant atomic properties for the present work are the average number of electrons, $N(\Omega)$, from which the atomic net charge, $q(\Omega)$, can be calculated as $Z_\Omega - N(\Omega)$, Z_Ω being the nuclear charge of the atom. AIM theory permits the identification of reactive sites by means of the Laplacian of the charge density, $\nabla^2\rho$. AIM defines the valence-shell charge concentration (VSCC) as the outer molecular zone where $\nabla^2\rho < 0$. This zone is the one which, upon chemical combination, is distorted to yield nonbonded critical points (NBCP), which are minima in $\nabla^2\rho$ (maxima of charge concentration), corresponding in number and position to the electron pairs defined by the Lewis and related models.[11,17] NBCP correspond to zones where an electrophilic attack can occur.

Results and Discussion

The Connectivity. The optimized geometries of the 1,2,3,4-thiatriazole-5-thiolate anion, $CS_2N_3^-$ (**1**), the hydracid, $HN_3SC{=}S$ (**2**), the interpseudohalogen, $CS_2N_3{-}CN$ (**3**), the methylazidodithiocarbonate, $CH_3CS_2N_3$ (**4**), the chloroazidodithiocarbonate, $ClCS_2N_3$ (**5**), and the fluoroazidodithiocarbonate, FCS_2N_3 (**6**), calculated at the B3LYP/6-31G** level of theory, are shown in Figure 1, and the bond lengths are indicated. The calculated parameters are in very good agreement with the available experimental data and theoretical results reported by Crawford et al.[3,7] (Table 1).

The five-membered ring is the standard form for the $CS_2N_3^-$ anion and its derivatives. The planarity of the $CS_2N_3^-$ anion is an indication for both the aromatic and pseudohalide character of this species.[3] Table 2 lists relevant topological properties obtained from this study. The topological analysis of BCPs in ρ of $CS_2N_3^-$ anion, **1**, and the covalent derivatives, **2**−**6**, reveal that all bonds forming the five-member ring correspond to covalent interactions, namely, a relatively large value for ρ_b and a negative value for $\nabla^2\rho_b$. The $|\lambda_1|/\lambda_3$ quotient is appreciably greater than 1, except for the N_1-N_2 bond for which these values are near 1. The ellipticities of bonds forming the ring have considerably large numerical values, and it reveals their partial double bond character due to the electronic charge delocalization over the ring surface. The G_b/ρ_b relationship is lower than 1 as usual in covalent bonds.

The exocyclic C−S bond is described by lower values of ρ_b, and $\nabla^2\rho_b$ shows small although negative values. The $|\lambda_1|/\lambda_3$ quotient is always more than 1 for the C_1-S_2 bonds. A remarkable situation lies in the HCS_2N_3 compound, **2**, in which the Laplacian of the electronic density, $\nabla^2\rho_b$, shows a small, positive value at the BCP. In the same way, the $|\lambda_1|/\lambda_3$ quotient is less than 1, and the G_b/ρ_b relationship is > 1. These topological properties reflect the bond polarity. Figures 2 and 3 show the $\nabla^2(\mathbf{r})$ contour maps for structures **1**−**3** and **4**−**6**, respectively, which clearly show the concepts previously mentioned. It can be seen that the interaction pattern of the ring atoms is nearly the same and clearly suggests the presence of shared interactions.

The same situation is found in the exocyclic bonds which exhibit a region of charge concentration along each bond, a characteristic feature associated with shared interactions. Nevertheless, it is necessary to highlight the interaction

Table 2: Topological Analysis of BCP in ρ of 1,2,3,4-thiatriazole-5-thiolate Anion, $CS_2N_3^-$ (**1**), Hydracid, $HN_3SC{=}S$ (**2**), Interpseudohalogen, $CS_2N_3{-}CN$ (**3**), Methylazidodithiocarbonate, $CH_3CS_2N_3$ (**4**), Chloroazidodithiocarbonate, $ClCS_2N_3$ (**5**), and Fluoroazidodithiocarbonate, FCS_2N_3 (**6**)[a]

	$C_1{-}S_2$	$C_1{-}N_1$	$C_1{-}S_1$	$S_1{-}N_3$	$N_1{-}N_2$	$N_2{-}N_3$	$N_1{-}H$	$S_2{-}C_2$	$C_2{-}N_4$	$C_2{-}H$	$S_2{-}X$
						1					
ρ_b	0.2065	0.3385	0.1943	0.1979	0.3804	0.4340					
$\nabla^2\rho_b$	−0.2846	−0.9986	−0.2941	−0.3149	−0.7416	−0.9551					
$\lvert\lambda_1\rvert/\lambda_3$	1.6724	1.9937	1.1137	1.1896	0.9122	1.0352					
ϵ	0.0693	0.1366	0.1834	0.1783	0.0914	0.1630					
G_b/ρ_b	0.7956	0.6015	0.3258	0.4502	0.5315	0.6062					
						2					
ρ_b	0.2166	0.3040	0.2014	0.1956	0.3680	0.4626	0.3387				
$\nabla^2\rho_b$	0.0295	−0.7912	−0.3452	−0.3129	−0.7017	−1.1329	−1.7923				
$\lvert\lambda_1\rvert/\lambda_3$	0.4718	1.6004	1.2901	1.2041	0.9131	1.1507	1.5992				
ϵ	0.0313	0.0775	0.2111	0.1893	0.1406	0.1910	0.0493				
G_b/ρ_b	1.2175	0.7006	0.3173	0.4484	0.5084	0.6215	0.1291				
						3					
ρ_b	0.1948	0.3670	0.2115	0.2002	0.3656	0.4510		0.2096	0.4688		
$\nabla^2\rho_b$	−0.3473	−1.0768	−0.3928	−0.3111	−0.6834	−1.0553		−0.4705	−1.0728		
$\lvert\lambda_1\rvert/\lambda_3$	1.3505	2.0007	1.6079	1.1400	0.8734	1.0848		4.0575	0.5338		
ϵ	0.2198	0.2107	0.2315	0.1841	0.0621	0.1586		0.3118	0.0156		
G_b/ρ_b	0.2849	0.7185	0.3679	0.4500	0.5141	0.6159		0.4575	1.7325		
						4					
ρ_b	0.2027	0.3589	0.2096	0.1945	0.3647	0.4551		0.1738		0.2774	
$\nabla^2\rho_b$	−0.3953	−1.0517	−0.3816	−0.2777	−0.6762	−1.0758		−0.2525		−0.9351	
$\lvert\lambda_1\rvert/\lambda_3$	1.7716	2.000	1.5023	1.0445	0.8712	1.0966		1.0133		1.4081	
ϵ	0.2524	0.1761	0.2139	0.1803	0.0653	0.1610		0.0739		0.0127	
G_b/ρ_b	0.3360	0.6859	0.3530	0.4427	0.5155	0.6206		0.2636		0.1432	
						5					
ρ_b	0.2093	0.3636	0.2099	0.1967	0.3604	0.4559					0.1677
$\nabla^2\rho_b$	−0.4140	−1.0712	−0.3829	−0.2895	−0.6527	−1.0808					−0.0327
$\lvert\lambda_1\rvert/\lambda_3$	1.6161	2.0165	1.5487	1.0765	0.8611	1.0992					0.6225
ϵ	0.3068	0.1884	0.2216	0.1800	0.0673	0.1605					0.3410
G_b/ρ_b	0.3000	0.6525	0.3654	0.4474	0.5172	0.6210					0.8777
						6					
ρ_b	0.2024	0.3642	0.2099	0.1995	0.3633	0.4529					0.1302
$\nabla^2\rho_b$	−0.3795	−1.0715	−0.3826	−0.3083	−0.6674	−1.0651					−0.0379
$\lvert\lambda_1\rvert/\lambda_3$	1.5006	2.0060	1.5377	1.1339	0.8679	1.0908					0.5957
ϵ	0.2647	0.1917	0.2238	0.1829	0.0674	0.1605					0.1064
G_b/ρ_b	0.3033	0.7024	0.3628	0.4493	0.5172	0.6180					0.3771

[a] ρ_b and $\nabla^2\rho_b$ in au.

pattern in the $S_2{-}X$ bonds in structures **5** and **6**, because of the electronegativity difference between the S and F and Cl atoms, respectively.

Regarding the situation related with the site of protonation in the HCS_2N_3 compound, that is to say, whether the site of protonation was at the exocyclic sulfur atom or at one of the ring nitrogen atoms (see Chart 1), the isomer with $N_1{-}H$ connectivity (**2**) was found to be the lowest energy isomer for HCS_2N_3 in the gas phase and the isomer with an exocyclic S−H bond (**2′**) was calculated to be the next higher energy isomer.[3] However, there is still no answer to the question about why the N−H isomer is the favored structure, in opposition to the higher stability of those covalent derivatives with an exocyclic S−R bond (R=CH_3, X, CN). To look for an answer to this question we also performed topological calculations on both structures (**2** and **2′**).

The results show that the higher stability of the covalent derivatives with S−R connectivites instead of N−R connectivity is due to a steric reason. It seems that the substituent bond to the exocycle sulfur has "more space" than the bond to the nitrogen of the ring. Obviously, we cannot use the same reasoning for the hydrogen atom. Thus, which would be the reason that makes the hydracid more stable with N−H connectivity?

Up to now, our calculations have allowed us to find two alternative explanations regarding the following aspects:

1. The proton affinity calculated by Crawford et al.[3] of 327.0 kcal mol^{-1} is similar to the proton affinity calculated[3] for the HCl of 339.3 kcal mol^{-1} (experimental[18] 333.2 kcal mol^{-1}). These values indicate that hydracid is a strong acid. If this is true, its anion (conjugate base) is weak and, therefore, more stable when it is dissociated.

2. The contour map of the Laplacian of the distribution of the charge density of the hydracid with N−H connectivity is much more similar to the contour map of the anion (at least more similar than the map of the hydracid with the

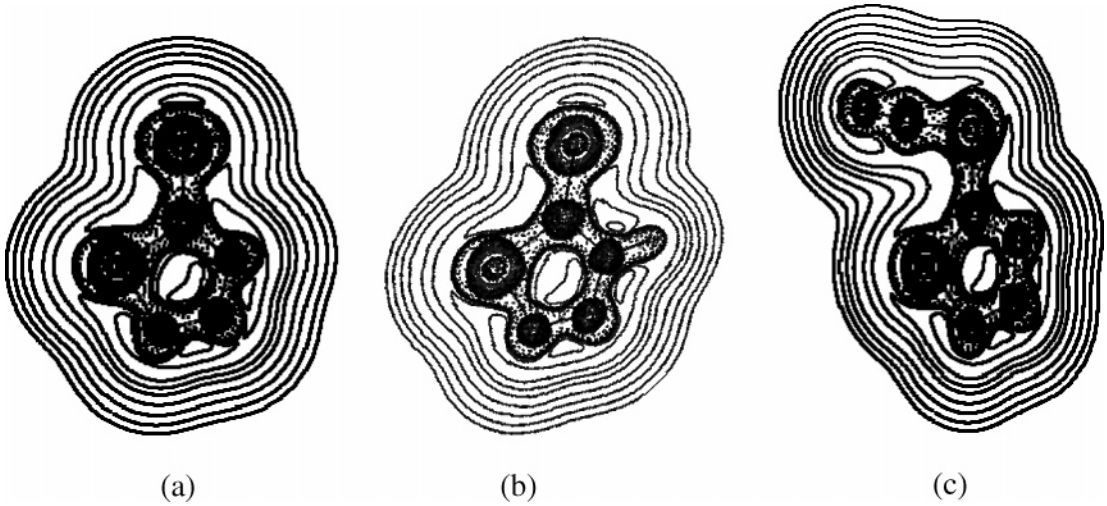

Figure 2. Laplacian of the electronic density of (a) 1,2,3,4-thiatriazole-5-thiolate anion, $CS_2N_3^-$ (**1**), (b) hydracid, $HN_3SC{=}S$ (**2**), and (c) interpseudohalogen, $CS_2N_3{-}CN$ (**3**), in the plane of rings. Broken lines denote regions of electronic charge concentration, and solid lines represent regions of electronic charge depletion. BCP are indicated with black circles. The molecular graphs are also indicated. The contours of the Laplacian of the electronic density increase and decrease from a zero contour in steps of ± 2, ± 4, $\pm 8 \times 10^n$, with n beginning at -3 and increasing by unity. The same set of contours is used in all the figures of the present work.

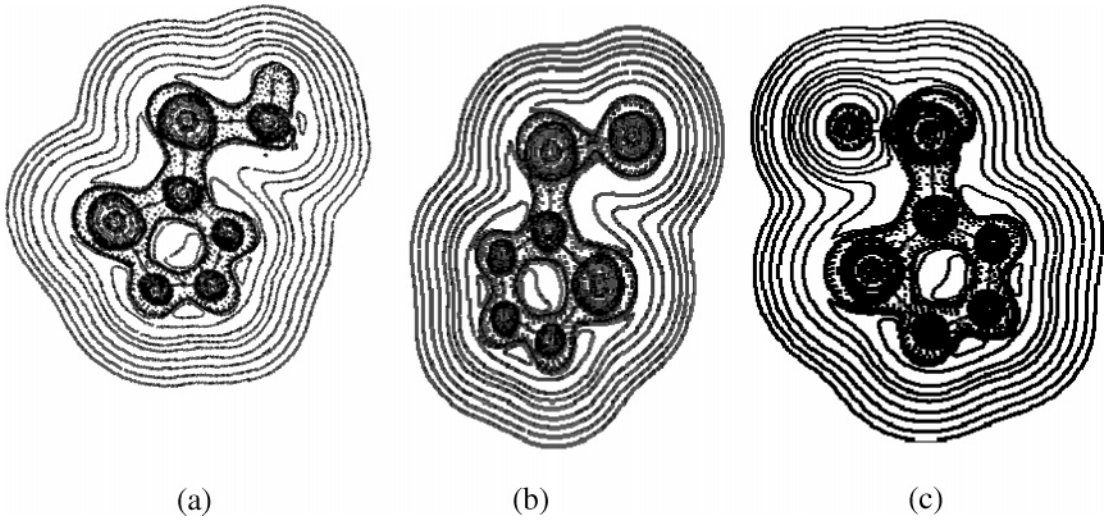

Figure 3. Laplacian of the electronic density of (a) methylazidodithiocarbonate, $CH_3CS_2N_3$ (**4**), (b) chloroazidodithiocarbonate, $ClCS_2N_3$ (**5**), and (c) fluoroazidodithiocarbonate, FCS_2N_3 (**6**), in the plane of rings. Broken lines denote regions of electronic charge concentration, and solid lines represent regions of electronic charge depletion. BCP are indicated with black circles. The molecular graphs are also indicated.

Chart 1: HCS_2N_3 Isomers with N−H Connectivity (**2**) and with an Exocyclic S−H Bond (**2′**)

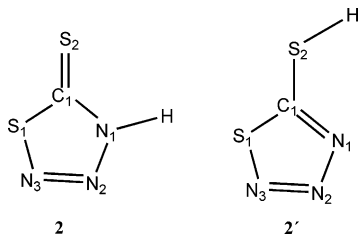

S−H connectivity) which could indicate that after the loss of the proton an anion is formed practically without changes in the electronic distribution. This feature can be seen when confronting the map of structure **2** (Figure 2b) with the map of structure **2′** (Figure 4).

Table 3: Net Charges, $q(\Omega)$, on Five-Member Rings and Exocyclic Sulfur Atoms for All Studied Structures[a]

	1	**2**	**2′**	**3**	**4**	**5**	**6**
q(C1)	+0.074	−0.055	+0.232	+0.264	+0.209	+0.238	+0.246
q(N1)	−0.608	−0.707	−0.601	−0.598	−0.608	−0.604	−0.605
q(N2)	−0.094	−0.007	−0.017	−0.003	−0.020	−0.003	−0.007
q(N3)	−0.456	−0.329	−0.326	−0.336	−0.335	−0.334	−0.344
q(S1)	+0.286	+0.476	+0.461	+0.539	+0.187	+0.520	+0.509
q(S2)	−0.199	+0.166	+0.214	+0.524	+0.457	+0.737	+0.380

[a] The units are atomic units.

Charge Distribution. The atomic charge polarizations which take place with chemical bonding are of fundamental interest to chemists. Therefore, to study the charge distribution that takes place with the intensity and direction of the

Table 4: Values of Laplacian of the Charge Density, $\nabla^2\rho$ [au], at the Nonbonded Critical Points (NBCP) of the Selected Atoms in Studied Structures[d]

atom	1	2	2′	3	4	5	6
N1	−2.7012 (1)[b]	−1.6284 (2)[a]	−2.8106 (1)[b]	−2.8427 (1)[b]	−2.8063 (1)[b]	−2.8078 (1)[b]	−2.8101 (1)[b]
N2	−3.0714 (1)[b]	−3.1253 (1)[b]	−3.1009 (1)[b]	−3.1459 (1)[b]	−3.0975 (1)[b]	−3.1279 (1)[b]	−3.1427 (1)[b]
N3	−2.7039 (1)[b]	−2.9092 (1)[b]	−2.9011 (1)[b]	−2.9203 (1)[b]	−2.8916 (1)[b]	−2.8651 (1)[b]	−2.8771 (1)[b]
S1	−0.4786 (2)[c]	−0.5026 (2)[c]	−0.4641 (2)[c]	−0.4619 (2)[c]	−0.4667 (2)[c]	−0.4689 (2)[c]	−0.4668 (2)[c]
S2	−0.4619 (2)[b]	−0.4883 (2)[b]	−0.5464 (2)[c]	−0.5627 (2)[c]	−0.5556 (2)[c]	−0.6728 (2)[c]	−0.6117 (2)[c]

[a] NBCP position: top and down of plane. [b] NBCP position: in plane. [c] NBCP position: top and down plane in sp^3 hybridization. [d] Numbers in parentheses indicate the NBCP encountered.

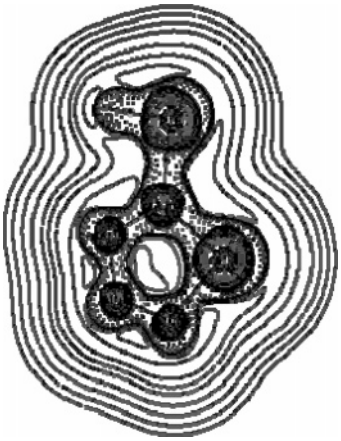

Figure 4. Laplacian of the electronic density of HCS_2N_3 isomers with an exocyclic S−H bond (**2′**), in the plane of ring. Broken lines denote regions of electronic charge concentration, and solid lines represent regions of electronic charge depletion. BCP are indicated with black circles. The molecular graphs are also indicated.

charge transfer, the net charges, $q(\Omega)$, were computed. Table 3 summarizes the atomic charges on five-member rings and on exocyclic sulfur atom for the structures studied (**1**−**6**). These results show that exocyclic S atom possesses a negative charge only in the anion, structure **1**, although practically the whole negative charge is located at the N1 atom. In structures **3**−**6**, the exocyclic S atom carries a considerable positive charge taking into account structure **2** due to the charge transfer of the S atom toward the R groups (R=CN, CH_3, X).

It is interesting to note that the charge transfer is important in structure **5**, where the S atom is bonded to the F atom. This situation is clearly evidenced in the Laplacian of the electronic density distribution (Figure 3c). On the other hand, in all cases the cyclic S atom carries a positive charge, which is bigger in structure **3**. The considerable values of the positive charges in structures **3**, **5**, and **6** on the cyclic S atom reveal a decreased electronic population on this atom in derivatives where the R groups contain electronegative atoms. In all derivatives studied, the charge of the cyclic C atom is positive (about +0.2 au).

Sites of Electrophilic Attack. To gain more insight into the site of attachment of the R group is most likely at the exocyclic sulfur atom in contrast to the N−R connectivity in the HCS_2N_3 compound, we undertook a topological analysis of the Laplacian of the electronic density. Therefore, NBCPs have been determined on the sulfur and nitrogen atoms value for all the studied structures.

Results are collected in Table 4. A single NBCP is found at the pyridine nitrogen N1, N2, and N3 in **1** and **3**−**6**. Those NBCP are coplanar with the ring. On the other hand, two NBCP are found for the amine nitrogen N1 in 2. The first of these NBCP is located at the apex of the pyramidic nitrogen (the place where the lone electron pair is usually represented). The second NBCP appears pointing toward the base of the pyramid. The values of $\nabla^2\rho$ in both NBCP are similar. The existence of these two NBCP can be explained in light of the conjugation between the amine group and the pseudoaromatic ring. In the absence of conjugation we can expect a single local maximum of charge concentration, a NBCP, corresponding to the lone electron pair located in a hybrid orbital pointing to the apex of the pyramid. However, when the amine group is conjugated with the aromatic ring, the electron pair is more similar to a two-lobed p orbital than to a hybrid orbital with a single lobe.

On the cyclic sulfur atom two NBCP are found, compatible with two lone electron pairs localized at the upper and lower positions of the plane corresponding to a sulfur atom with sp^3 hybridization. At the same time, on the exocyclic sulfur atom bound to the C atom in the ring are found two NBCP located in the plane, compatible with two lone electron pairs corresponding to a sulfur atom with sp^2 hybridization in structures **1** and **2**. On the other hand, in the other ones the two lone electron pairs are placed in two sp^3 hybrid orbitals.

In all studied cases the nitrogen atoms have $\nabla^2\rho$ values of the NBCP larger than those of the sulfur atoms. When the values of $\nabla^2\rho$ are compared at the different nonbonded critical points on N atoms of the studied species, the NBCP at the N2 exhibits the highest concentration of charge (see Table 4). Provided that $\nabla^2\rho$ can be considered as an indicator of the site electrophilic attack, the center with the highest $\nabla^2\rho$ value seems to correspond to the preferred attack site.

The data analysis of Table 2 shows clearly that the hydracid N−H has in the exocyclic S atom the same array of lone electron pairs corresponding to a hybridization approximately sp^2 (two lone electron pairs in the plane and with an angle of 155.5°). This point can reinforce what was pointed out with regard to the connectivity since in the hydracid S−H: the exocycle S atom has a hybridization of approximately sp^3 (two lone electron pairs up and down the molecular plane and forming between them an angle of 134.4°). Then, with the loss of the proton it would be possible to undergo a rehybridization to sp^2 when forming the anion. Looking at what happens with the nitrogen atom of the ring which is bonded to the hydrogen atom in the hydracid N−H (**2**), this atom has two NBCP: one up and another down the

plane and forming an angle of only 8° with the N atom, resembling a pure p orbital, while the N atom maintains the sp^2 hybridization. We believe that this situation allows maintaining the aromatic character of the species, and, therefore, with a single change in the electronic distribution, the N atom reorders a single NBCP.

Conclusions

We have undertaken a topological analysis of the so-called "azidodithiocarbonate" anion, 1,2,3,4-thiatriazole-5-thiolate anion, $CS_2N_3^-$ (**1**), and its covalent derivatives: the hydracid, $HN_3SC{=}S$ (**2**), the interpseudohalogen, $CS_2N_3{-}CN$ (**3**), the methylazidodithiocarbonate, $CH_3CS_2N_3$ (**4**), the chloroazidodithiocarbonate, $ClCS_2N_3$ (**5**), and the fluoroazidodithiocarbonate, FCS_2N_3 (**6**).

The results reveal that all bonds forming the five-member ring correspond to covalent interactions. The higher stability of the covalent derivatives with S−R connectivites instead of the N−R connectivity is explained on the basis of an existing steric reason. Additionally, the distribution of the charge density of the hydracid with N−H connectivity and the anion seem to indicate that after the loss of the proton the anion is formed practically without changes in the electronic distribution. In this way, with a single change in the electronic distribution the N atom reorders two at a single NBCP.

A remarkable result of this work, merging from this analysis, is that the nitrogen atoms are sites that exhibit the highest concentration of electronic charge. The topological studies have shown that they are useful and effective tools for elucidating the structures of many CS_2N_3-containing species.

Acknowledgment. The authors acknowledge the Supercomputer Center of the Secretary for the Technology, Science, and Productive Innovation, Argentina, for computational time. N.B.O. thanks the Facultad de Agroindustrias and SECYT UNNE for financial support. A.H.J. is a member of the Carrera del Investigador CIC, Buenos Aires, and E.A.C. and N.B.O. are members of the career researcher of CONICET, Argentina.

References

(1) (a) Greenwood, N. N.; Earnshaw, A. A. In *Chemistry of the Elements*; Pergamon Press: Oxford, U.K., 1984. (b) Klapötke, T. M.; Janiak, C.; Meyer, H.-J. In *Modern Inorganic Chemistry*; Walter de Gruyter: Berlin, 1998.

(2) Birkenbach, L.; Kellermann, K. *Ber. Dtsch. Chem. Ges.* **1925**, *58B*, 786.

(3) Crawford, M.-J.; Klapotke, T. M.; Mayer, P.; Vogt, M. *Inorg. Chem.* **2004**, *43*, 1370−1378.

(4) Sommer, F. *Ber. Dtsch. Chem. Ges.* **1915**, *48*, 1833.

(5) Perman, C. A.; Gleason, W. B. *Acta Crystallogr*. **1991**, *C47*, 1018.

(6) (a) Browne, A. W.; Hoel, A. B. *J. Am Chem. Soc*. **1922**, *44*, 2315. (b) Howlett-Gardner, W.; Browne, A. W. *J. Am Chem. Soc*. **1927**, *49*, 2759. (c) Smith, G. B. L.; Wrattman, P.; Browne, A. W. *J. Am Chem. Soc*. **1930**, *52*, 2806.

(7) (a) Crawford, M.-J.; Klapötke, T. M. *J. Fluorine Chem*. **1998**, *92*, 153−156. (b) Crawford, M.-J.; Klapötke, T. M. *Inorg. Chim. Acta* **1999**, 294, 68−72. (c) Crawford, M. J.; Klapötke, T. M.; Klüfers, P.; Mayer, P.; White, P. S. *J. Am. Chem. Soc*. **2000**, *122*, 9052.

(8) Okulik, N.; Jubert, A. H.; Castro, E. A. *J. Mol. Struct. (THEOCHEM)* **2002**, *589-590*, 79−87.

(9) Lieber, E.; Offentdahl, E.; Rao, C. N. R. *J. Org. Chem*. **1963**, *28*, 194.

(10) (a) Hohenberg, P.; Kohn, W. *Phys. Rev.* **1964**, *136B*, 864. (b) Kohn, W.; Sham, L. J. *Phys. Rev.* **1965**, *140A*, 1133. (c) Parr, R. G.; Yang, W. *Density Functional Theory of Atoms and Molecules;* Oxford University Press: Oxford, 1989.

(11) (a) Bader, R. F. W. *Atoms in Molecules. A Quantum Theory*; Clarendon: Oxford, 1990. (b) Popelier, P. L. A. *Atoms in Molecules. An Introduction;* Pearson Education: Harlow, U.K., 1999.

(12) Frisch, M. J.; Trucks, G. W.; Schlegel, H. B.; Scuseria, G. E.; Robb, M. A.; Cheeseman, J. R.; Zakrzewski, V. G.; Montgomery, J. A., Jr.; Stratmann, R. E.; Burant, J. C.; Dapprich, S.; Millam, J. M.; Daniels, A. D.; Kudin, K. N.; Strain, M. C.; Farkas, O.; Tomasi, J.; Barone, V.; Cossi, M.; Cammi, R.; Mennucci, B.; Pomelli, C.; Adamo, C.; Clifford, S.; Ochterski, J.; Petersson, G. A.; Ayala, P. Y.; Cui, Q.; Morokuma, K.; Malick, D. K.; Rabuck, A. D.; Raghavachari, K.; Foresman, J. B.; Cioslowski, J.; Ortiz, J. V.; Stefanov, B. B.; Liu, G.; Liashenko, A.; Piskorz, P.; Komaromi, I.; Gomperts, R.; Martin, R. L.; Fox, D. J.; Keith, T.; Al-Laham, M. A.; Peng, C. Y.; Nanayakkara, A.; Gonzalez, C.; Challacombe, M.; Gill, P. M. W.; Johnson, B. G.; Chen, W.; Wong, M. W.; Andres, J. L.; Head-Gordon, M.; Replogle, E. S.; Pople, J. A. *Gaussian 98, revision A.6*; Gaussian, Inc.: Pittsburgh, PA, 1998.

(13) Becke, A. D. *J. Chem. Phys.* **1993**, *98*, 5648.

(14) Lee, C.; Yang, W.; Parr, R. G. *Phys. Rev. B* **1988**, *37*, 785.

(15) Huzinaga, S.; Andzelm, J.; Klobukowski, M.; Radzio-Andzelm, E. Sakai, T.; Tatewaki, H. *Gaussian Basis Set for Molecular Calculations*; Elsevier: Amsterdam, 1984.

(16) Biegler-König, F. W.; Bader, R. F. W.; Tang, T. H. *J. Comput. Chem.* **1982**, *13*, 317.

(17) Bader, R. F. W. *Chem. Rev.* **1990**, *91*, 893.

(18) NIST Service. Web-book. http://www.nist.gov (accessed Nov 10, 2005).

CT0503062